



Synthesis of PAN-nanofibers for the separation of aqueous pollutants and performance of the net-zero energy water treatment plant

Ibrahim M. Alarifi^a, Mohammad Kashif Uddin^{b,c,*}, Ahmed Bilal Awan^d, Mu. Naushad^e, Abdulaziz R. Alharbi^f, Ramazan Asmatulu^g

^aDepartment of Mechanical and Industrial Engineering, College of Engineering, Majmaah University, Al-Majmaah 11952, Saudi Arabia, email: i.alarifi@mu.edu.sa (I.M. Alarifi)

^bDepartment of Chemistry, College of Science, Majmaah University, Zulfi Campus, Al-Zulfi 11932, Saudi Arabia, emails: mohdkashifchem@gmail.com/m.kashifuddin@mu.edu.sa (M.K. Uddin)

^cBasic Engineering Sciences Department, College of Engineering, Majmaah University, Al-Majmaah 11952, Saudi Arabia

^dDepartment of Electrical Engineering, College of Engineering, Majmaah University, Al-Majmaah 11952, Saudi Arabia, email: a.awan@mu.edu.sa (A.B. Awan)

^eDepartment of Chemistry, College of Science, Bld#5, King Saud University, Riyadh 11451, Saudi Arabia, email: mnaushad@ksu.edu.sa (M. Naushad)

^fDepartment of Mechanical Engineering, Fahad Bin Sultan University, Tabuk 71454 Saudi Arabia, email: dr.aralharbi@gmail.com (A.R. Alharbi)

^gDepartment of Mechanical Engineering, Wichita State University, 1845 Fairmount, Wichita, Kansas 67260, email: ramazan.asmatulu@wichita.edu (R. Asmatulu)

Received 29 December 2019; Accepted 2 May 2020

ABSTRACT

This study presents the multidisciplinary studies and combined different types of work in an approach intended to solve the research problems including (i) the synthesis of polyacrylonitrile (PAN)-nanofibers using the electrospinning method; (ii) characterization of the produced nanofibers using scanning electron microscopy, microscopic characterization, Fourier transform infrared spectroscopy, thermogravimetric analysis, and contact angle and wetting properties; (iii) the removal of various micropollutants present in dam water and wastewater via the nanofiltration process, (iv) design and performance evaluation of a local sewage water treatment plant, and (v) analysis of the photovoltaic-based net-zero energy system for the Tabuk water treatment plant.

Keywords: Polyacrylonitrile (PAN)-nanofibers; Nanofiltration; Wastewater; Net-zero energy water treatment plant; Economic analysis

1. Introduction

The presence of micropollutants is common in water streams and is the primary cause of polluted drinking water sources. There are many types of micropollutants in groundwater, surface water, wastewater, and even in drinking water at low levels (micro to nano range). Micropollutants consist of various inorganic and organic compounds that

enter the aqueous environment because of industrial discharge and domestic use of cosmetics, drugs, and textile products. Most are persistent and hazardous and cannot be removed by using the conventional water treatment process. They have chronic health effects on living beings and their continuous expulsion can cause long-term harm to society. Treatment processes such as adsorption [1–7], ion exchange [8–10] coagulation [11], reverse osmosis [12],

* Corresponding author.

and photodegradation [13,14] have been reported for the removal of various aqueous pollutants. The nanofiltration process is a separation practice that is used for desalination applications and removing various micropollutants, radionuclides, bacteria, and viruses [15]. This membrane-based process provides better results during the industrial separation process than other available techniques such as reverse osmosis, ultrafiltration, etc. [16]. Nanofiltration membranes are capable of decreasing the hardness, nitrates, sulfates, total dissolved solids, turbidity, color, and a reasonable amount of salt from aqueous streams [17].

Saudi Arabia is exploring renewable methods of water treatment and funding many projects related to desalination and water purification. Groundwater is the primary source of drinking water in Saudi Arabia and there is a need for an advanced water treatment process to meet international standards. Polymeric nanofibers are a modern material providing excellent results as a filtration membrane for treated water [18–20]. Polymeric fiber composites have significant physiochemical properties and various industrial applications. Because of their non-corrosive nature, lightweight, inexpensiveness, easy handling, and high specific and tensile strength, they can be used in the construction of aircraft, chemical equipment, and other civil and mechanical engineering setups. There are many methods to prepare nanofibers. Electrospinning is a unique, fast, and economical technique that can produce highly porous nanofibers at a high production rate. Electrospun nanofibers have potential applications in the environmental, medical, biotechnology, defense, and energy production fields [21]. Electrospun nanofibers are an active research field in material science and engineering applications [22]. In this research work, the synthesis of polyacrylonitrile (PAN) nanofibers (PAN-NF) was conducted using the electrospinning procedure. PAN-NF was then utilized as a filtration membrane to remove pollutants in dam water and wastewater. To facilitate the filtration process, the different weight of the polymeric solution of polyvinylpyrrolidone (PVP) and antibacterial Garamycin was encapsulated to improve the bioactivity of the nanofibers. The nanomembrane was characterized using various techniques to analyze the physio-chemical properties of PAN-NF before and after the filtration process.

This study also presents the engineering design of the Tabuk sewage treatment plant (TSTP), Saudi Arabia, and its performance in increasing the water means of the state. We aimed to address the issue of water treatment by determining a feasible and efficient water treatment process. An advanced water treatment process was conducted to eliminate inorganic ions (calcium (Ca^{2+}), magnesium (Mg^{2+}), sulfate (SO_4^{2-}), nitrates (NO_3^-), chloride (Cl^-), and fluoride (F^-)), alkalinity, turbidity, and silica and reduce pH, total dissolved solids (TDS), total coliform, and bacteria (*Escherichia coli*) from dam and wastewater samples. The effect of TSTP in desalination was observed after testing the concentration of the essential inorganic ions and other water quality parameters in the influent and effluent. The wastewater was treated through various stages of the TSTP. Chemical, physical, and bacterial analysis of influent and effluent water samples were also conducted.

A solar-energy-based net-zero energy (NZE) system was proposed for the TSTP. A stand-alone system needs energy

storage units to avoid power fluctuations due to intermittent solar resource [23]. The NZE solar-based system on the other hand is directly connected to the grid and it does not need energy storage units, therefore, NZE systems are gaining popularity in developed countries [24]. In the NZE system, a sufficient amount of renewable energy is generated onsite such that the energy purchased from the grid is equal to the energy sold to the grid. NZE systems have many advantages over off-grid energy systems. The energy storage for off-grid systems needs a high installed capacity to serve the required electric load because the energy needs to be stored for later use. An NZE system solves this problem. In an NZE system, a grid is used for storage. During the time when renewable energy is available, the excess energy is sold to the grid, and during the time when the renewable energy resource is unavailable, the required load is served by importing energy from the grid. In this study, a photovoltaic-based NZE water treatment plant is proposed. The reason for selecting a photovoltaic-based NZE water treatment plant is the abundant availability of solar energy in this region [25].

Several research questions were developed such as (i) what is the impact of the PAN-nanofiber membrane in the nanofiltration of polluted water samples?, (ii) what is the performance of the Tabuk sewage treatment plant in treating wastewater and how can it be improved?, (iii) how can one obtain clean water using clean energy in a water treatment plant?, to answer these questions several research aims were also developed such as (i) synthesizing PAN-nanofibers and analyzing dam water and wastewater samples, (ii) evaluating the impact of PAN-nanofibers in water purification of dam and wastewater as a filtration membrane using a filtration setup, (iii) assessing the engineering design of the Tabuk sewage treatment plant and the chemical, physical, and bacterial properties of influent and effluent water samples, and (iv) designing and analyzing of the photovoltaic (PV)-based NZE system. We propose the use of potential PAN-NF in water treatment plants as a filtration membrane as the result of this study proving its capacity in filtering micropollutants from dam and wastewater. This is the first study analyzing an NZE system for a water treatment plant and proposing PAN-NF as a filtration membrane for water purification in water treatment plants.

2. Materials and methods

2.1. Materials and instrumentation

PAN (molecular weight: 53.06 g/mol), PVP (molecular weight: 111.14 g/mol), dimethylformamide (DMF), and Garamycin sulfate (GS) were supplied in the purity range by Sigma-Aldrich (United States) and directly used. Several devices from the Hach Company, USA were used to measure water quality parameters. The TDS and conductivity were measured using a Hach Sens ION5 while pH was measured using a Hach Sens ION3. A HatchHQ30d was used to measure the DO in the water samples. Total suspended solids (TSS), chemical oxygen demand (COD), and turbidity were measured using a HatchDR/890 colorimeter. A HatchDR/2010 spectrophotometer was used to measure alkalinity and ammonia. Ion chromatography (Metrohm Company, Switzerland) was

used to measure anions and cations (SO_4^{2-} , NO_3^- , F^- , Cl^- , Ca^{2+} , and Mg^{2+}). A Lovibond incubator and HachBODTrak were used to measure biochemical oxygen demand (BOD). Various steps of the Quanti-Tray/2000 technique were conducted to identify *E. coli* and coliform in the dam and wastewater.

2.2. Water treatment plant

2.2.1. General information

The TSTP is in Tabuk, Saudi Arabia. The plant site is between the latitude 28.5712178 and longitude 36.623858. Figs. S1a and S1b show the geographical location and aerial view of the TSTP. The plant is designed to handle a hydraulic capacity of 90,000 m^3/d (average). However, the plant is currently treating 130,000 m^3/d of municipal wastewater because of the pollution load. The wastewater is typically received via two main lines transferring domestic sewage. Flow is monitored as each line is equipped with an electromagnetic flowmeter. Part of the flow is received via trucking and tankering. As per data collected, this part represents approximately 1.8% (2% is considered) of the total actual received daily flow. A degreaser (solvent containing cleaning agent) is employed with this part and then all water is mixed in one collection chamber before screening. The effluent

line from the degreaser to the influent collection chamber is equipped with two electromagnetic flowmeters.

The electricity consumption per cubic meter of water treatment is 0.24 kWh/m^3 , and the average electrical load of the plant is 31,507 kWh/d . The monthly electricity consumption is shown in Fig. 1a. The electrical load of the plant is relatively higher during the summer because of the air conditioning load of the plant. This region has a very high level of global horizontal irradiance (GHI). The average GHI in this region is 6.31 $\text{kWh}/\text{m}^2/\text{d}$. The monthly average GHI, clearness index, and temperature variations at the plant site are shown in Fig. 1b.

2.2.2. Process description

Fig. 2 shows the layout/process flow diagram of the TSTP. The plant consists of two phases identical to each other regarding their general treatment scheme (Fig. 2). Phase 1 was designed to serve approximately 300,000 pop equivalent (PE) with a total capacity of 60,000 m^3/d . The treatment scheme is a typical conventional treatment scheme that consists of screening and a grit removal system serving as the primary treatment followed by the secondary treatment of a complete mix biological treatment system (aeration and settling). The secondary effluent then passes through a gravity

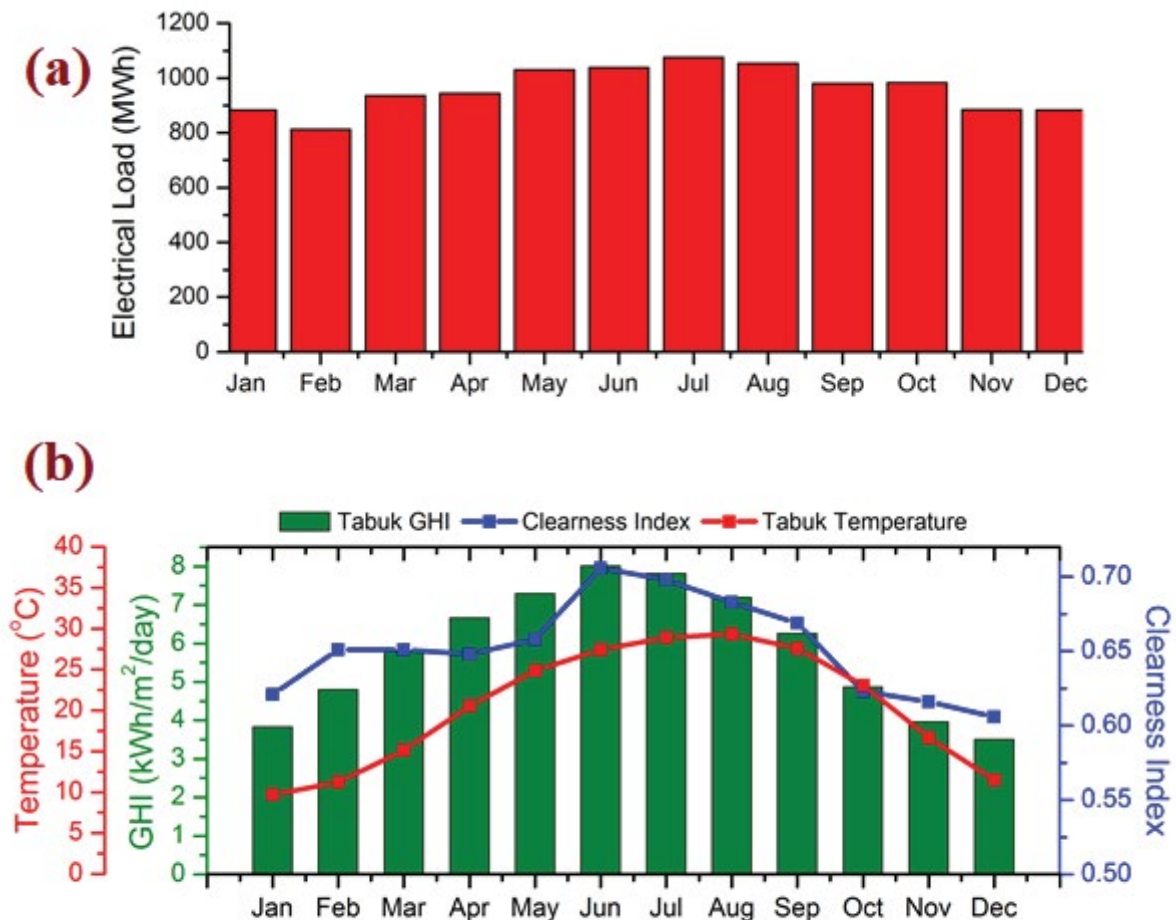


Fig. 1. (a) Monthly electrical load profile and (b) solar resource data.

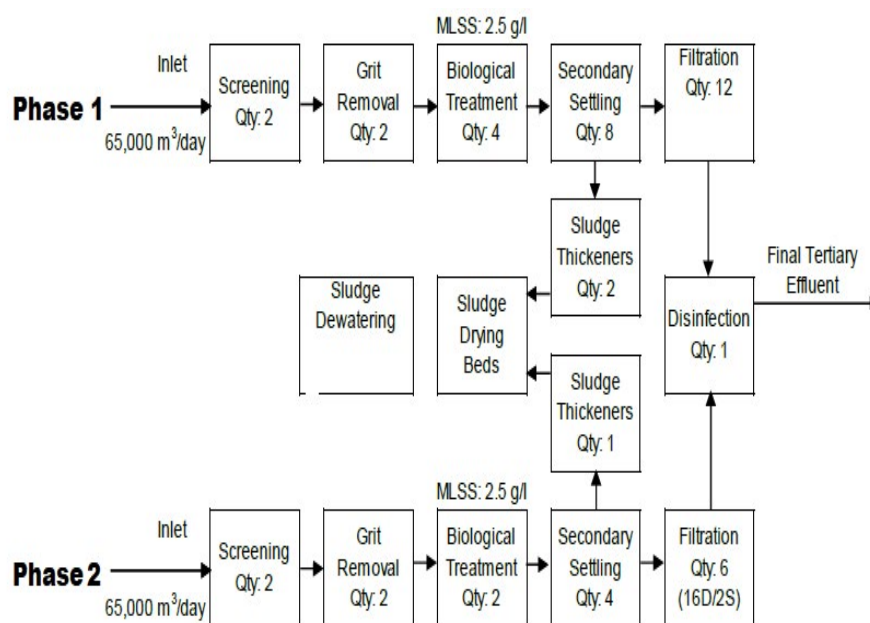


Fig. 2. Layout process phase diagram of TSTP.

filtration system as a final polishing step. Finally, the treated effluent is chlorinated using chlorine gas. Collected sludge is sent to two gravity thickeners before being sent to open drying beds. The initial design includes a complete sludge drying system that consists of two belt presses with sufficient space for future expansion, polymer preparation, a dosing system, and finally a dewatered sludge conveying system. Phase 2 was designed to serve approximately 150,000 PE with a total capacity of 30,000 m³/d of wastewater with the same treatment scheme. The flow is equally circulated between the two phases at 65,000 m³/d. The pre-treatment facility is equipped with a pH meter, conductivity meter, DO meter, TSS meter, and electromagnetic flowmeters at the pump station. Electrical energy is consumed throughout the TSTP to meet the operational power demand of the treatment facilities as well as administrative and utility facilities. According to information provided by the O&M contractor (Almoussa operating company, Saudi Arabia), power consumption is monitored by Saudi Electric Company, Saudi Arabia (SEC) averaging 31,507 kWh/d during 2018. Emergency power is available via diesel power generators that can provide 100% standby power needed to operate the whole treatment plant according to the O&M contractor. The generators are periodically run, tested, and maintained to ensure their standby operability. The electrical power generation in Saudi Arabia is fossil fuel-based resulting in considerable emission to the environment. Therefore, an NZE system for the water treatment plant is proposed.

2.2.3. Description of phase design

The design of the TSTP is divided into the following three phases:

- *Primary treatment* – Fine screening is mandatory to remove fine solids that may negatively affect the treatment

units downstream. This phase considers the service water cleaning system. The cleaning system includes a service water tank, high-pressure pumps, and solenoid valves. The system can serve the mechanical screens, screening conveyor, compactor, and all other parts of the screening facilities. The grit removal system is a squared horizontal type. The provided settling area is sufficient to serve the design capacity (60,000 m³/d). The oil and grease collection tank is equipped with submersible pumps, flow measuring devices, and level detection devices.

- *Secondary treatment* – This includes biological treatment consisting of four aeration tanks. Phase 1 is a complete mix system. The objective is the removal of organic materials (BOD/COD/total organic carbon) and nitrification (ammonia oxidation). Secondary clarification is conducted using eight clarifiers in Phase 1 and four clarifiers in Phase 2, each having a diameter of 28 m and consequently an area of 616 m² (total active area: 7,392 m²). The clarifiers are equipped with scraping mechanisms and surface skimmers.
- *Tertiary treatment* – Sand gravity filters are fed by submersible pumps, each with a capacity of 706 L/s. Phase 1 has 12 filtration cells, each 17 m × 3 m. Phase 2 has six cells of the same dimensions. The chlorination process is conducted through direct injection of prepared chlorine solution into the outlet of the tertiary filters. The chlorine solution preparation consists of chlorinators, evaporators, injectors, and water booster pumps. The system is also equipped with residual chlorine analyzers and chlorine leak detector instruments. The thickening unit consists of 2 and 1 picket fence thickeners 20 m in diameter for phase 1 and phase 2, respectively. Sludge drying beds are available to store and dry excess sludge. Collected supernatant is sent to the inlet works of the TSTP. The use of the drying beds has a direct impact on

the surrounding areas such as the emission of unpleasant odors and fly swarms. The drying beds, if well managed, can be used as a temporary solution to reduce the load on the thickeners. The dewatering facility consists of a dewatering start-up and running the dewatering machines which aids in decreasing the loads on the sludge thickeners. Table 1 lists the equipment installed in the TSTP. Fig. 3 shows the water treatment process in the TSTP.

2.3. Wastewater treatment

The wastewater influent is passed through the TSTP, Tabuk, Saudi Arabia. Physical, chemical, and biological processes are used to analyze various water quality parameters or contaminants such as TDS, TSS, COD, BOD, dissolved oxygen (DO), conductivity, total nitrogen (TN), total alkalinity, turbidity, pH, total coliform bacteria, phosphate ions (PO_4^{3-}), oil, and grease. The wastewater properties were then determined before and after each phase of the TSTP. The treated safe water as effluent is released into the environment.

2.4. NZE water treatment plant

An NZE water treatment plant is a grid-connected plant that has onsite renewable energy generation. NZE is achieved by producing sufficient onsite electrical energy such that the net energy imported from the grid is equal to the net energy exported to the grid. An NZE water treatment plant is achieved by employing a grid-connected PV system. The electrical output of the PV system depends on the temperature, solar radiation, and other factors such as dust and ground reflectance. The PV output is calculated using the following expression [26]:

$$P_{PV} = \eta_{PV} A_{PV} G_T \quad (1)$$

where η_{PV} is the efficiency of the PV system, G_T is the GHI hitting the PV cells, and A_{PV} is the area of the PV arrays. The efficiency of the PV system is provided as follows [27]:

$$\eta_{PV} = \eta_r \eta_{pc} \left[1 - \alpha_p (T_c - T_{c,STC}) \right] \quad (2)$$

Table 1
List of equipment installed in TSTP

Process stage	Equipment	Type	Total installed (phase 1 and 2)
Inlet works	Degreasing system	Floating type	1
	Pump station, lifting pumps	Submersible	3
	Fine screens	NA	NA
	Coarse screens	Motorized	4
	Screening conveyors	Belt type	2
	Screening compactors	NA	NA
Preliminary treatment	Grit removal	Elevator mech.	4
	Grit tank aeration system	NA	NA
	Grit removal scrapping bridge	Low speed geared scrapper mechanism	4
	Grit classifier	NA	NA
	Primary classifier scrapping bridge	NA	NA
	Primary sludge transfer pumps	NA	NA
Secondary treatment	Aeration tanks	Fixed high speed surface aerator	26
	Secondary settling tanks	Classical gravitational circular clarifiers	12
Tertiary treatment	Chlorine dosing system	Gas chlorination	1
	Filtration cells	Sand filtration	18 cells
Sludge treatment	Sludge recycling pumps	Archimedean screw, submersible	3, 4
	Sludge thickeners	Gravity circular thickeners	3
	Thickened sludge transfer pumps	Screw	2
	Drain pumps	Submersible	3
	Sludge dewatering system	Medium pressure belt press, polymer dosing system, dewatering cleaning pumps, shaftless screw conveyors	2, 1, 3, 1
Odor control unit	Pretreatment	Activated carbon filter, fouled air fan, air ducts, and cover	2, 2, 2

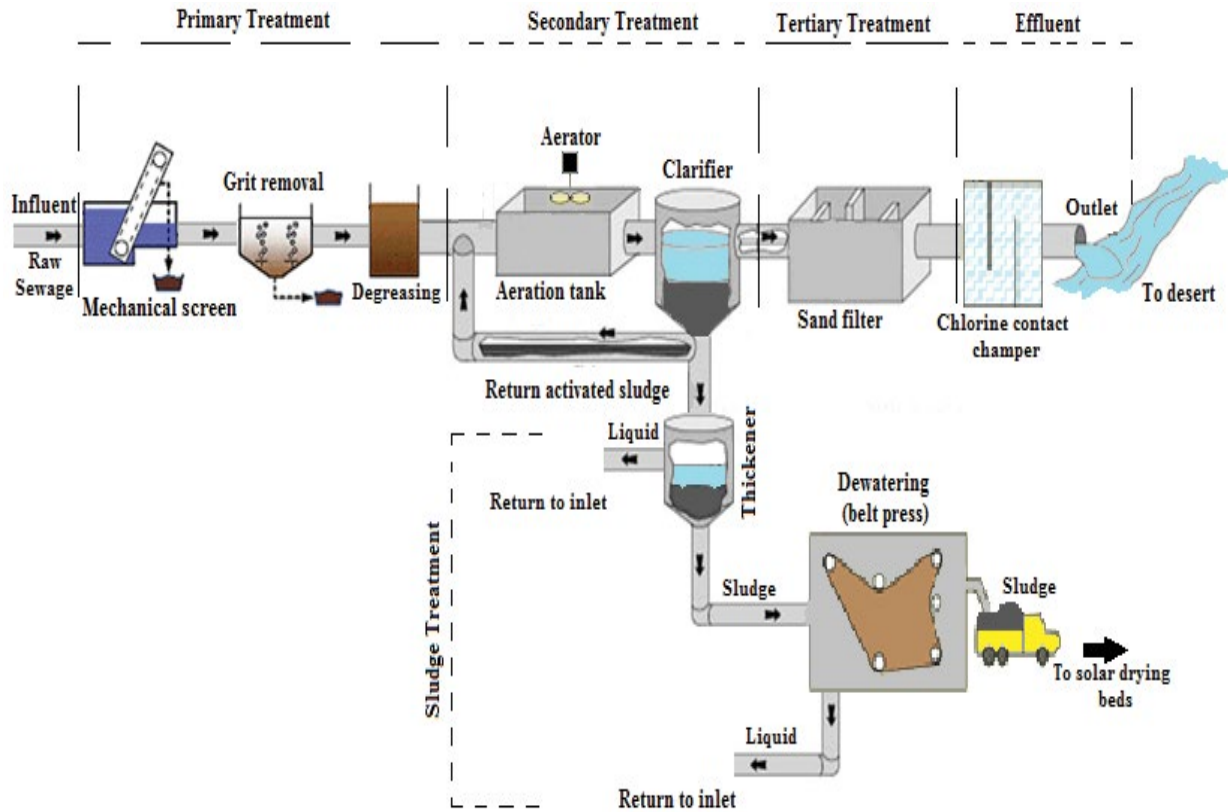


Fig. 3. Description of the water treatment process in TSTP.

where η_r is the reference module efficiency, α_p is the temperature coefficient of power, T_c is the PV cell temperature, $T_{c,STC}$ is PV cell temperature at standard test conditions, and η_{pc} is the maximum power point tracking (MPPT). The PV cell temperature is given as follows [28]:

$$T_c = \frac{T_{amb} + (T_{c,NOCT} - T_{a,NOCT}) \left(\frac{G_T}{G_{T,NOCT}} \right) \left[1 - \frac{\eta_{mp,STC}(1 - \alpha_{TP} T_{c,STC})}{\tau \alpha_a} \right]}{1 + (T_{c,NOCT} - T_{a,NOCT}) \left(\frac{G_T}{G_{T,NOCT}} \right) \left(\frac{\alpha_p \eta_{mp,STC}}{\tau \alpha_a} \right)} \quad (3)$$

where T_{amb} is the ambient temperature, $T_{c,NOCT}$ is the nominal operating cell temperature (NOCT), $T_{a,NOCT}$ is the ambient air temperature at NOCT, G_T is GHI on PV module, $G_{T,NOCT}$ is solar radiation at NOCT (1 kW/m²), α_p is temperature coefficient of power, $\eta_{mp,STC}$ is maximum power point efficiency at STC, α_a is solar absorbance and, τ is solar transmittance.

The annual energy output of the PV system is provided as follows [29]:

$$E_{PV} = \sum_{n=1}^{8760} P_{PV}(n) \quad (4)$$

The system advisor model (SAM) by the national renewable energy laboratory (NREL) was used to design the PV system [30]. SAM makes performance predictions and cost of energy estimates for grid-connected power projects

based on installation and operating costs and system design parameters that are specified by the user as inputs to the model. Canadian solar CS6U-340M PV modules were employed for this NZE plant. The characteristics of the PV module and system converter are provided in Table 2. The design parameters of the NZE system are shown in Table 3. The typology of the PV plant in this research work is a ground-mounted installation of parallel PV arrays. The NZE water treatment plant was compared to the existing conventional plant. The comparison was made based on the Levelized cost of energy (LCOE) and greenhouse gas emission.

2.5. Synthesis of polymeric nanofibers

In this study, PAN (2 g) was dissolved in DMF (18 g) at a percentage weight ratio of 10/90. Then, 5% each of PVP and Garamycin was supplemented into the PAN/DMF combination. Garamycin is an antibacterial antibiotic used to decrease membrane biofouling, killing viruses and bacteria, while PVP is a fining agent used to enhance the rate filtration rate. Homogeneous mixtures were formed by shaking on a magnetic stirrer for 30 min at 60°C at 450 rpm and were used for the synthetic process.

During the electrospinning process, PAN and PAN/5%PVP+5%Garamycin solution were completely mixed into a 10 mL syringe of polymeric solution which was then transferred in a 0.5 mm syringe pump (KD Scientific Company, United States) at a flow pumping rate of approximately 2 mL/h. One end of the 0.25 mm copper electrode needle

was connected to a high DC supply at 25 kV and the other end of the copper electrode was installed to the syringe. Approximately 22 cm distance was maintained between the capillary needle tube and aluminum collector target, which was attached with an aluminum sheet. Fig. 4 shows the experimental setup for the electrospinning process. The prepared electrospun nanofibers were dried 18 h before removing them from the aluminum foil.

2.6. Characterization

The characterization of the prepared pure PAN-nanofibers (PAN-NF) and blended PAN with PVP and

Garamycin-PAN/5%PVP+5%Garamycin (bPAN-NF) was conducted using various techniques. Scanning electron microscopy (SEM) and microscopic images of PAN-NF and bPAN-NF were observed to determine the morphology, fiber diameter, and any significant effect in the nanofibers before and after filtration of the polluted dam and wastewater samples. Fourier transform infrared spectroscopy (FTIR) was used to identify the compounds and chemical interaction on the surface of the studied polymeric nanofibers (before and after filtration process) at a different wavelength. The water contact angles of the PAN-NF were determined to understand the behavior of

Table 2
Characteristics of the PV module

Description	Specification
PV module electrical data at standard testing conditions (STC)	
Nominal efficiency	18.16%
Maximum power (P_{mp})	350 Wdc
Maximum power voltage (V_{mp})	38.3 Vdc
Maximum power current (I_{mp})	9.1 Adc
Open circuit voltage (V_{oc})	46.6 Vdc
Short circuit current (I_{sc})	9.7 Adc
Temperature coefficient of power (α_{TP})	-0.423°C
Lifetime	25 y
Inverter characteristics	
Efficiency	98%
Maximum AC power	59.859 kW
Maximum DC power	61.1 kW
Nominal AC voltage	400 V
Nominal DC voltage	629.26 V
Maximum DC voltage	1,000 V
Maximum DC current	110 A
Minimum MPPT DC voltage	570 V
Maximum MPPT DC voltage	800 V
Lifetime	15 y

Table 3
Design parameters of the NZE system

Description	Specification
Size of the PV system to achieve NZE	7,250 kW
PV modules	
Number of PV modules	20,720
Strings in parallel	2,072
Modules per string	10
Total module area	41,616.6 m ²
String open circuit voltage	462 V
String maximum power voltage	379 V
Inverter	
Total capacity	6,019 kW _{ac}
Total capacity	60,264 kW _{dc}
Number of inverters	132
Maximum DC voltage	480 V
Minimum MPPT DC voltage	300 V
Maximum MPPT DC voltage	480 V
Overall system	
De-rating factor	90%
Ground reflectance	30%
System performance annual degradation	0.5%

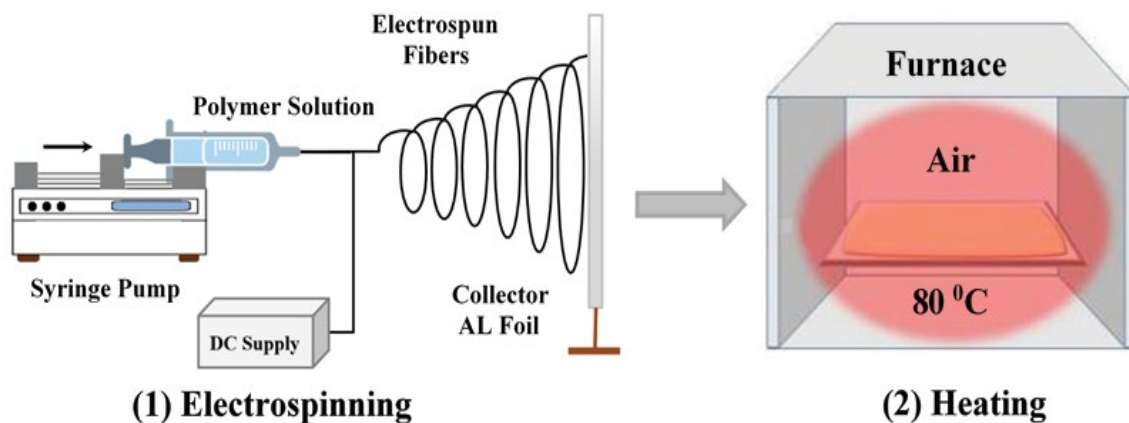


Fig. 4. Experimental setup for the electrospinning process.

the solid surface with water droplets. Thermogravimetric analysis (TGA) was measured over time (50°C–400°C).

2.7. Aqueous samples and nanofiltration

Two different water samples (dam water and wastewater) were collected. The 200 m-long and 7 m high Alzraib dam in Alzraib valley, Saudi Arabia, was chosen to collect dam water as the water that passes through this valley contain sand, mud, and rocks making it rich in salt and silica content. The nanofiltration process was conducted by passing the dam and wastewater through the nanomembranes (electrospun nanofibers) under pressure created by using a vacuum during the filtration setup. Fig. 5 shows the instrumental setup used for the filtration process. The purpose of this work was to separate the suspended solids and inorganic micropollutants to disinfect and soften the water samples (dam and wastewater).

3. Results and discussion

3.1. Characterization

3.1.1. SEM and microscopic images

The diameter and morphology of PAN-nanofibers were observed via SEM and are shown in Figs. 6a–d. The average diameter of the fine thread-shaped fiber structure of pure PAN-NF was 827.1 nm (Fig. 6a). The diameter of the PAN-NF persisted nearly unchanged after the addition of PVP and Garamycin (5% each). However, the use of PVP at a higher concentration could expand the average diameter of PAN-NF because of the increase in internal friction of the PAN chemical precursor. In addition, the morphology of the PAN-NF threads seemed to be slightly rougher and had more grooved surfaces with crinkles and folds after the addition of PVP and Garamycin (Fig. 6b). Figs. 6c and d show SEM images of the PAN-NF after filtration of dam water and wastewater, respectively. The suspended

and colloidal particles are visible in these figures and can be precisely detected. However, after wastewater filtration more solid particulates adhere to the surface of PAN-NF in comparison to that of the dam water. The PAN-NF surface microstructure was brightly charged after filtration; this morphological change was because of the collection of particulate matter. Therefore, the results suggested that the prepared PAN-NF can be potentially used to reject colloids, micro and macromolecules, suspended particles, viruses, bacteria, and other compounds.

The optical microscopic images of PAN-NF show the smooth surface in which significant quantities of larger-diameter fibers are noticeably (Fig. 7a). Figs. 7b and c show that the PAN-NF after successful filtration of dam water and wastewater consisted of aggregates of inorganic particles.

3.1.2. Fourier transform infrared spectroscopy

Fig. 8a shows the FTIR spectra of PAN-NF before and after filtration of the dam water. In pure PAN-NF (before filtration), two narrow peaks at 2,920 and 2,847 cm^{-1} were recognized as CH_2 functional groups in PAN [31] and a C–H stretching vibration [32], respectively. The band at 1,670 cm^{-1} corresponds to the C=O stretching (acidic, H-bonded) vibration [33] while the band at 1,456 cm^{-1} corresponds to CH_2 bending [33]. The lower intensity peaks at 1,065 and 546 cm^{-1} are complex and assigned to C=O twisting [31]. The additional peaks (3,697 and 3,404 cm^{-1}) and the shifting of the main characteristic peaks in the FTIR spectrum of the dam water filtered PAN-NF suggest successful micropollutant removal. The peak at 2,933 cm^{-1} in the FTIR spectra of PVP- and Garamycin-blended PAN-NF (mPAN-NF) is the characteristic peak for the $-\text{CH}_2$ ν -CH groups of PVP [34]. The peak at 2,245 cm^{-1} indicates the presence of nitrile ($\text{C}\equiv\text{N}$) bonds in the PAN chain [35]. The PVP spectrum shows its mark at 1,657 and 1,284 cm^{-1} in the form of CO and C–N, respectively [36]. As shown in Fig. 8b, some peaks shifted to a lower wave number indicating bond weakening.

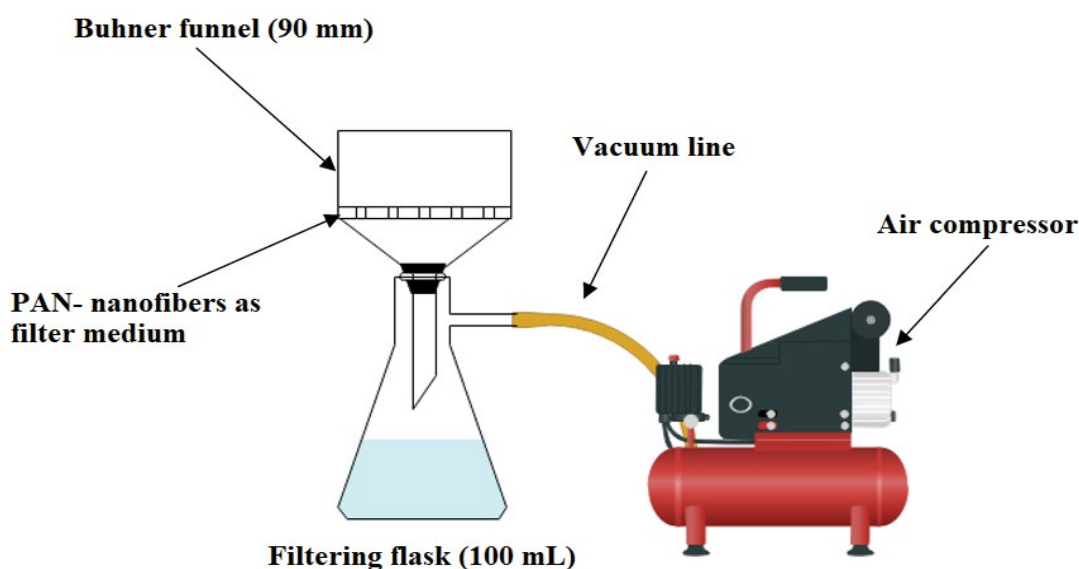


Fig. 5. Instrumental setup for the filtration process.

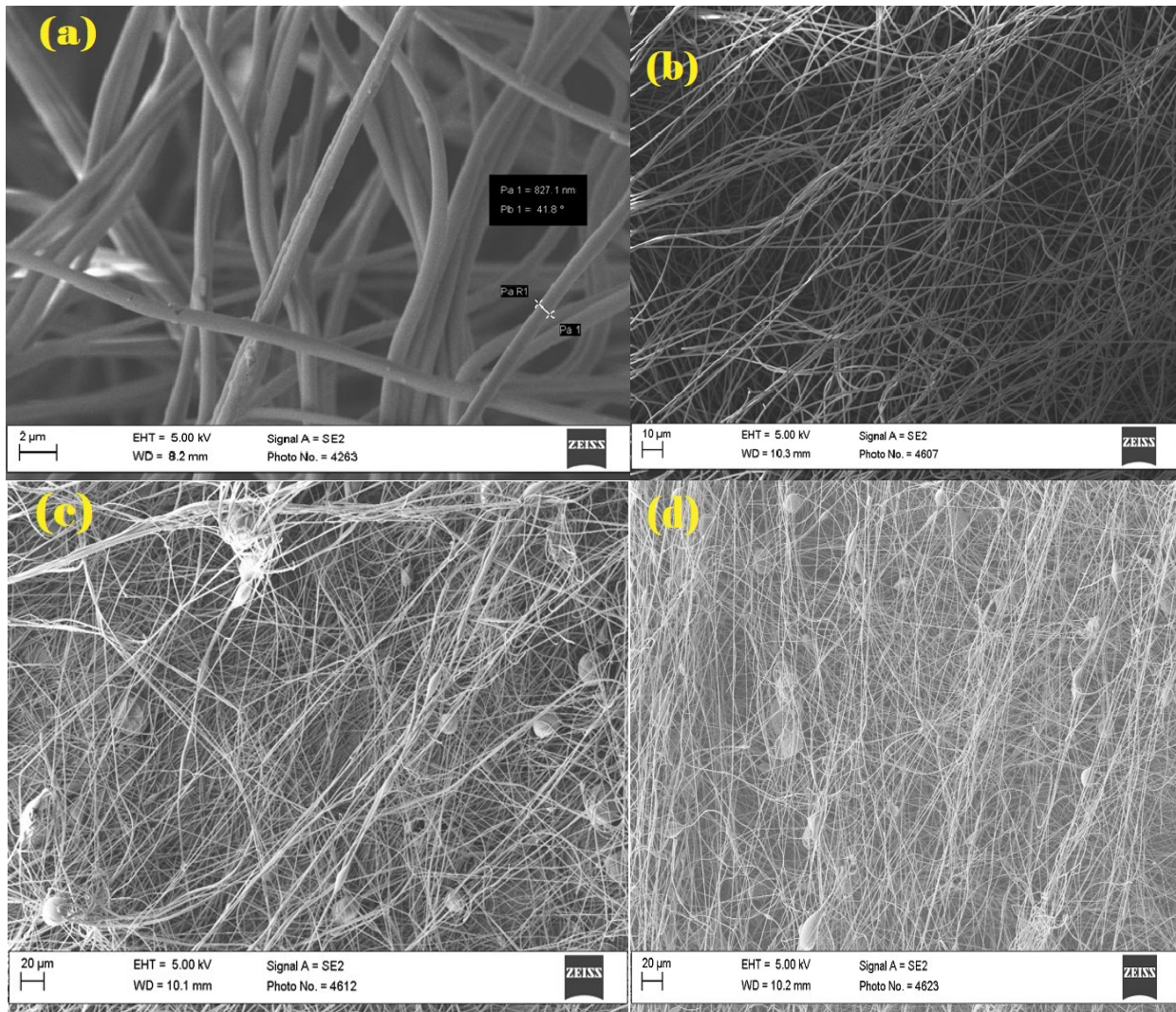


Fig. 6. SEM images of (a) pure PAN-nanofibers, (b) PVP and Garamycin blended PAN-NF (*t*-PAN-NF), (c) PAN-NF after filtration of dam water, and (d) PAN-NF after filtration of wastewater.

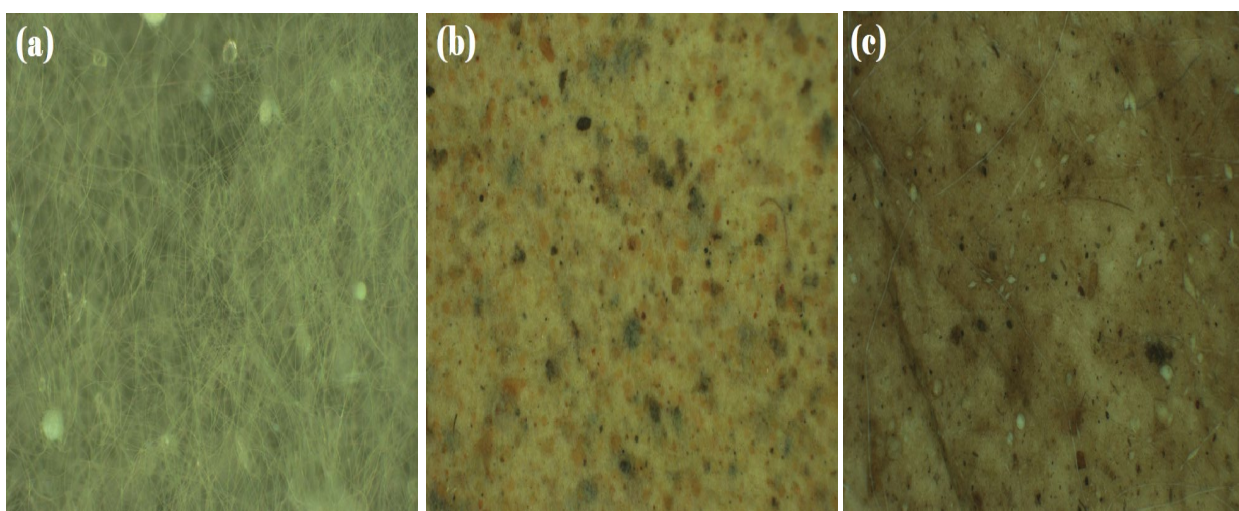


Fig. 7. Microscopic images of (a) pure PAN-NF, (b) PAN-NF after filtration of dam water, and (c) PAN-NF after filtration of wastewater.

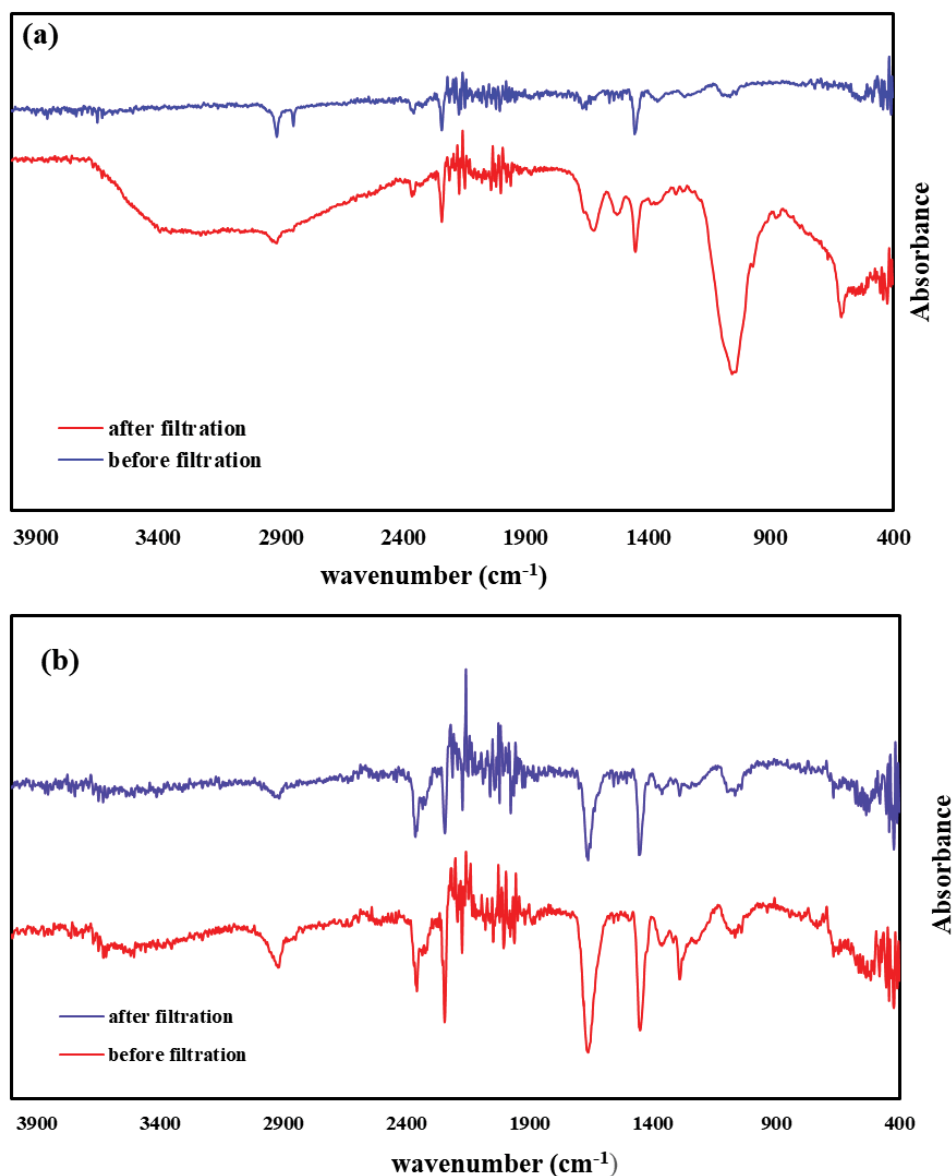


Fig. 8. (a) PAN-NF and (b) bPAN-NF before and after filtration of dam water.

These changes show the interaction between micropollutants and blended mPAN-NF.

3.1.3. Water contact angles

The static contact angles were measured for both PAN-NF and bPAN-NF to study the wetting tendency and surface tension of the material. As can be seen in the water contact angle of PAN-NF (Fig. 9a), the left side is 30.77° while the right side is 27.22° presenting a mean contact angle of 28.99° . These values ($<90^\circ$) mean that the PAN-NF surface is hydrophilic and thus interacts with liquid molecules in a favorable manner. The PVP addition makes PAN-NF more hydrophilic given its nature, and as shown in Fig. 9b, bPAN-NF has a contact angle of 22.69° at the left side and 23.32° at the right side resulting in a mean value of 22.96° .

It seems that Garamycin did not play any role in the wettability of the bPAN-NF surface (Fig. 9b).

3.2. Wastewater treatment at the TSTP

The wastewater treatment process at the TSTP was assessed by analyzing the concentration of water quality parameters before and after each stage. Table 4 presents the examined results for the wastewater sample. The analysis of the effluent shows that many essential water parameters were efficiently controlled during the water treatment process. The performance of the TSTP in controlling BOD, COD, TSS, turbidity, conductivity, pH, oil, and grease was found to be efficient as it managed to maintain the concentration of these water-related parameters within the regulation limit set by the Indian standard (IS) for drinking

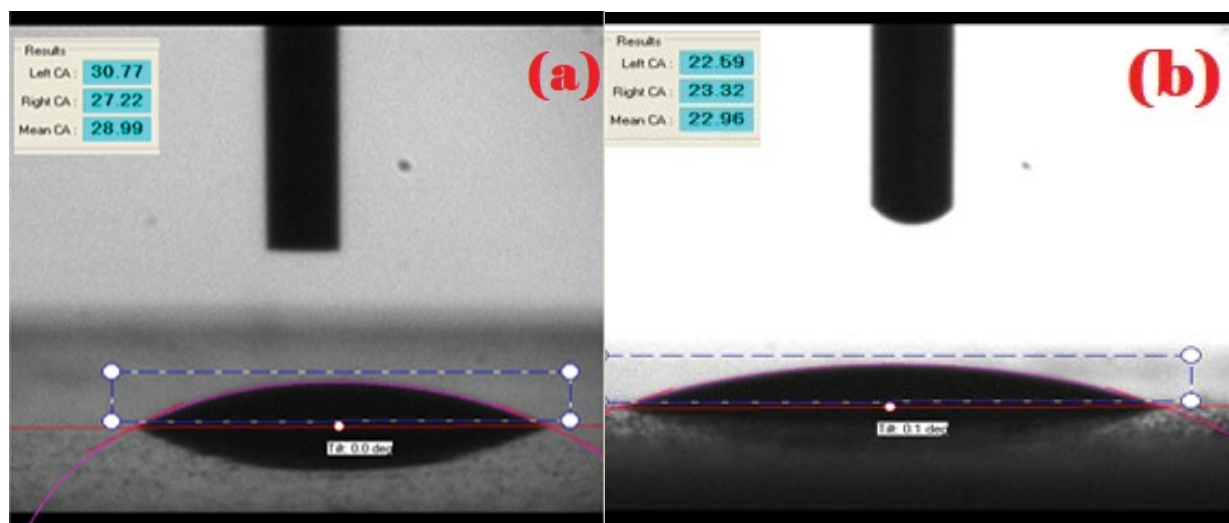


Fig. 9. Water contact angles of (a) PAN-NF and (b) bPAN-NF.

Table 4
Wastewater properties before and after each treatment stage in TSTP

Parameter	Influent maximum design	Influent	After secondary treatment	After tertiary treatment	% removal (Effluent)	Regulations	Comply
BOD (mg/L)	600	200	15	5	97.5	>30	Yes
COD (mg/L)	1,000	450	30	14	96.8	>40	Yes
TSS (mg/L)	500	200	18	6	98.0	10	Yes
TN (mg/L)	120	70	17	8	88.5	7	No
TDS (mg/L)	2,500	2,000	1,933	1,890	5.5	1,750	No
Turbidity (NTU)	500	251	18	7	97.2	40	Yes
Conductivity ($\mu\text{S}/\text{cm}$)	5,000	4,000	3,952	3,229	19.2	3,500	yes
pH	6–9	7.4–7.9	7.1	7.0	2.7	6–8.4	Yes
Oil–grease (mg/L)	100	53	5	0	100	52	Yes
$\text{NH}_3\text{-N}$ (mg/L)	100	50	15	7	86.0	5	No
PO_4^{3-} (mg/L)	45	38	13	11	75.5	NA	NA
Coliform (MPN/100 mL)	Un-limited	NA	55	50	9.0	2.2	No

water [37]. The percentage removal of these critical parameters between the treatment stages was excellent. Fig. S2 shows the wastewater in the influent and after the treatment stages. However, it can also be seen that the concentration levels of TN, TDS, and $\text{NH}_3\text{-N}$ in the effluent are slightly higher than the recommended limit and the TSTP failed to control total coliform. Based on these outcomes, an adequacy assessment of the TSTP was completed by local auditors to improve its wastewater treatment efficiency. According to the report prepared by the O&M contractor (Saudi Arabia), the following are the major issues during the treatment process:

Assessment

- The filtration facility in phases 1 and 2 needs some equipment replaced in addition to filtration media. This affects the performance of the TSTP and the amount of water introduced to each cell in addition to the inefficient backwash process.
- An automatic sampler should be installed at the inlet and the outlet of the water stream. It was recommended by the auditor to consider a new screening system including a new civil structure and all necessary accessories.
- There is no odor removal system to treat H_2S and other malodorous gases. High emissions of H_2S and other gases present serious health risks to TSTP personnel.
- A service water cleaning system should be provided. The system should be able to serve the mechanical screens, screening conveyor, compactor, and all other parts of the screening facility. The cleaning system should include – as a minimum requirement – a service water storage tank, high-pressure pumps, and necessary solenoid valves.
- The screening compactor and flow meters after the screens should be provided.
- The new disinfection/chlorination system should be able to automatically optimize the dosage rate and totalize the dosed chlorine.

- An additional thickener in phase 2 to reduce the solid load on the existing thickener should be installed.
- Drying beds can be used as an emergency system in case of any mechanical failure in the dewatering system.
- Wet scrubbers are the best solution; however, biological bio-filters followed by activated carbon are an alternative solution for odor treatment.
- A proper dewatering system should be provided and final disposal should be outside the plant premises.
- A SCADA control and monitoring system should be installed. It should cover all the plant stages, enabling monitoring of all operational parameters and allowing remote control. This would reduce manpower use and improve operational efficiency.
- The screening channels are not covered, it was recommended by the auditor to install a proper cover on the screening channels.
- According to the calculations performed, the aeration efficiency is low (1.12 kg O₂/kWh). As the BOD load in the aeration tanks is within design limits, in phase 1, it seems that either the aerator power is not sufficient or the aerator rotating tables are not sufficiently immersed in the water to provide optimal efficiency.
- It was recommended by the auditor to install a sludge balancing tank before the thickeners so that the sludge from phases 1 and 2 is combined in the tank and equally distributed between the thickeners. Currently, the thickener in phase 2 is quite heavily loaded as it is nearly handling the same amount of sludge as that of phase 1 but with one-half the thickeners. Mechanically, the phase 1 thickeners are in an acceptable condition and phase 2 thickener is in good condition.
- Lighting should be limited to where it is needed and solar-powered lighting should be introduced to conserve electrical power.

3.3. Nanofiltration of dam water and wastewater via NiO-NP

Compliance of raw and filtered dam water and wastewater samples.

3.3.1. Dam water

Table 5 presents the chemical and physical parameters' analysis of the dam water samples before and after nanofiltration. The pH value of raw dam water was found to be 7.90 while for the filtered water samples it varied from 7.10 to 7.00 for both the used nanofibers with an average value of 7.05. These results indicate that chemicals such as lime and granular chlorine in the raw dam water were successfully filtered by PAN-NF and bPAN-NF resulting in a pH decrease to a satisfactory level. The turbidity level of the raw water was 29.1 nephelometric turbidity units (NTUs) which exceeded the recommended limit of 1 NTU of Indian standard [37] and the Department of Water Affairs and Forestry (DWAF) [38] for domestic use. This high turbidity in the raw dam water could be because of dissolved sediments and may be associated with severe diseases. The turbidity levels of the final filtered water samples varied from 2.32 to 1.70 NTUs with an average value of 2.01 NTUs for both used PAN-nanofibers. The permissible turbidity in the filtered drinking water standards is 4 NTUs and less than 5 NTUs as per the European standards [39] and the World Health Organization [40], respectively. The results are promising as a 94.10% turbidity removal was obtained. These results also show the control of total hardness whose value was 446 mg/L but then decreased by as much as 75.5% to a mean value of 11.5, within the permissible limit as per the IS of drinking water [37]. In the case of inorganic ions, it was noted that the fluoride concentration in the dam water was found to be 1.60 mg/L which was on the edge of

Table 5
Chemical and physical analysis of filtered dam water samples

Water parameters	Analysis of raw dam water (before nanofiltration)	Analysis of treated dam water (after nanofiltration by NiO-NP)	Analysis of treated dam water (after nanofiltration by tNiO-NP)	Maximum % removal after nanofiltration
pH	7.9	7.1	7.0	11.3
Turbidity (NTU)	29.1	1.7	2.3	94.1
TDS (mg/L)	3,170	1,012	953	69.9
Ca ²⁺ (mg/L)	94.1	32.1	43.1	65.8
Mg ²⁺ (mg/L)	47.5	19.4	23.2	59.1
Total hardness	446	114	109	75.5
SO ₄ ²⁻ (mg/L)	72.2	11.5	12.3	84.0
NO ₃ ⁻ (mg/L)	2.9	0.4	0.9	86.2
F ⁻ (mg/L)	1.6	0.7	0.6	62.5
Cl ⁻ (mg/L)	1,786.1	847.1	870	52.5
Total alkalinity (mg/L)	134.6	52.4	53.9	61.0
Silica (mg/L)	76.44	18.5	22.2	75.7
Total coliforms (MPN/100 mL)	2,120	447.5	110.3	94.79
<i>E. coli</i> (MPN/100 mL)	14	5.9	0.9	93.57

the maximum limit in the drinking water [37]. The nanofiltration made it more suitable with an average value of 0.65 mg/L. The recommended limit for sulfate and calcium ions in drinking water is 200 mg/L [37]; the concentrations of both SO_4^{2-} and Ca^{2+} were found to be within the acceptable limit in both the raw and filtered water. However, PAN-NF and bPAN-NF showed efficiency in removing 84.00% and 86.20% of the SO_4^{2-} and Ca^{2+} , respectively. The magnesium (47.55 mg/L), chloride (1,786.10 mg/L), and TDS (3,170 mg/L) concentrations in the raw dam water were very high and could not be decreased to suitable limits via nanofiltration during the treatment process. The Mg^{2+} , Cl^- , and TDS mean values were 21.3, 858.55, and 982.5 mg/L, respectively. The SiO_2 content in the raw dam water was 86 mg/L; silica in natural water usually ranges up to 100 mg/L [26]. After nanofiltration by PAN-NF and bPAN-NF, the average values decreased to 11.90 mg/L, an excellent 75.70% decrease. It can be concluded that both nanomaterials (PAN-NF and bPAN-NF) worked well as filtration membranes and effectively cleaned most of the studied micropollutants to within allowable levels for drinking water.

In the case of bacterial analysis, the use of the Garamycin antibiotic proved remarkable in treating bacteria (coliform and *E. coli*) found in dam water as bPAN-NF showed a better excellent result in removing both from the dam water samples. The coliform and *E. coli* concentrations decreased up to 94.79% and 93.57%, respectively. The mean values were found to be 278.8 MPN/100 mL and 3.4, respectively, in the filtered water samples. The results confirm that both nanofibers can be effectively used in water treatment and bPAN-NF was more suitable for bacterial removal.

Fig. 10a shows the PAN-NF membrane before and after dam water filtration, while Fig. S3 shows the unfiltered and filtered dam water samples.

3.3.2. Wastewater

Table 6 presents the chemical, physical, and bacterial properties analysis of wastewater samples before and after nanofiltration using the PAN-NF and bPAN-NF membranes. The raw wastewater pH was found 7.95, the same as that of the dam water samples. After nanofiltration, the pH value varied from 7.10 to 7.00 for both used nanofiber membranes with an average pH value of 7.05 in the filtered wastewater samples. The turbidity level of the wastewater samples decreased up to a maximum of 84.09% after nanofiltration, slightly less than that of the dam water. However, the average value (8.05) of the turbidity was within the permissible limit. TDS also were within the permissible limit in the filtered wastewater samples (an average value of 1,145.0 mg/L) and less than the raw wastewater (1,558 mg/L). TSS in the raw wastewater samples were 37 mg/L, within the permissible limit. However, the nanofibers performed well to reduce the TSS by up to 81.08%; the average value was 10.0 mg/L. Total nitrogen (TN) and ammonia ($\text{NH}_3\text{-N}$) in the wastewater significantly decreased by up to 90.83% and 88.0% for PAN-NF and bPAN-NF, respectively. The presence of COD and BOD in the wastewater was controlled to a satisfactory level using the nanofiltration process. Significant performance of the PAN-nanofibers was obtained to remove oil and grease from raw water. A nearly 100% removal

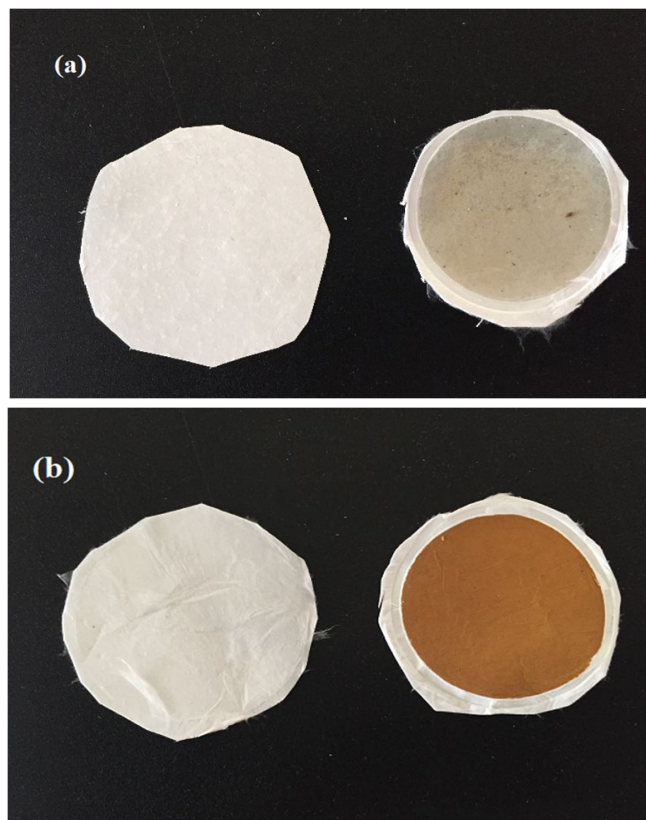


Fig. 10. PAN-NF before and after filtration of (a) dam water and (b) wastewater.

efficiency was achieved. The presence of bacterial organisms (coliform and *E. coli*) in the wastewater samples was detected. Again, the use of Garamycin provided an excellent result and decreased total coliform and *E. coli* levels by up to 95.60% and 97.05% for bPAN-NF.

Fig. 10b shows the PAN-NF membrane before and after dam water filtration, while Fig. S4 shows the unfiltered and filtered wastewater samples.

3.4. Energy and economic analysis

The proposed NZE water treatment plant was achieved by employing 7,250 kW of PV modules. The idea was to install sufficient PV modules to produce sufficiently excessive electricity that could be sold to the grid and bought back during the night when no sun is available. The hourly average energy analysis of the proposed NZE water treatment plant is shown in Figs. 11a–c. The PV energy output followed the GHI pattern (Fig. 1b). The PV energy output was higher during summer as compared to that during winter. Although the high temperature during the summer degrades PV performance, the very promising GHI level aids in achieving a better energy yield. It can be observed in Fig. 11a that the PV energy output is based on the load profile of the water treatment plant which is very useful to utilize the energy generated. Grid sales were higher during the summer while grid purchases were higher during the winter because of the low GHI leading to lower energy output from

Table 6
Chemical, physical, and bacterial analysis of filtered dam water samples

Water parameters	Analysis of raw wastewater (before nanofiltration)	Analysis of treated wastewater (after nanofiltration by NiO-NP)	Analysis of treated wastewater (after nanofiltration by tNiO-NP)	Maximum % removal after nanofiltration
BOD	19.0	9.3	8.1	57.59
COD	55.0	21.0	23.4	61.81
pH	7.9	7.1	7.0	11.39
Turbidity (NTU)	44.0	10.0	7.0	84.09
TDS (mg/L)	1,558.0	1,199.0	1,091.0	29.97
TSS (mg/L)	37	13	7.0	81.08
Ca ²⁺ (mg/L)	74.3	22.0	19.3	74.02
Mg ²⁺ (mg/L)	37.1	14.4	13.2	64.42
Total hardness	316	94	99	70.25
Total nitrogen	120	14	11	90.83
SO ₄ ²⁻ (mg/L)	67.4	13.5	7.9	88.27
NO ₃ ⁻ (mg/L)	3.3	1.4	0.9	72.72
F ⁻ (mg/L)	2.1	0.7	1.1	66.66
Cl ⁻ (mg/L)	786.5	247.1	270	68.58
PO ₄ ³⁻ (mg/L)	45	13	11	75.55
Total alkalinity (mg/L)	84.1	32.4	33.9	61.47
NH ₃ -N (mg/L)	100	12	12	88.00
Silica (mg/L)	31.44	6.2	6.9	80.27
Oil and grease	100	9	3	97.0
Total coliforms (MPN/100 mL)	1,820	214.5	80.3	95.60
<i>E. coli</i> (MPN/100 mL)	17	3	0.5	97.05

the PV system. Overall, the grid sales and purchases were equal throughout the year showing that an NZE system for the water treatment plant was achieved. The GHI, PV electrical output, electrical load, grid sales, and purchases for each hour of a typical summer and winter day are shown in Figs. 11b and c. PV energy output and grid sales were higher during the summer (Fig. 11b) as compared to those during the winter (Fig. 11c) because of the high GHI during the summer. PV energy output and grid sales on a typical winter day are lower during the early morning and evening. Overall, the energy imported from the grid is more than the energy sold to the grid on a typical winter day while for a typical summer day, even though the electrical load is higher the grid sales are more than grid purchases given the very good GHI resources during summer, which is in line with the load profile of the plant.

The economic analysis of the NZE system was performed based on the net present cost (NPC) and LCOE. The NPC was computed by adjusting the future revenue and costs during the total lifetime of the project to today's money value by applying a discounted rate. The discount rate for the proposed project was selected as 6% [41], and the lifespan of the project is 25 y. The costs of various components of the NZE system are tabulated in Table 7 [42,43]. The cost of energy for a governmental industry in Saudi Arabia is 8.5 ¢/kWh [42]. The NPC of the NZE system for the water treatment plant was calculated to be US\$ 10.7 million. The cost flow

summary of the system during the lifespan of the project is shown in Fig. 12a. The main share of NPC originates from the capital cost of the PV modules and the balance of the system equipment (US\$ 5.8 million) followed by grid purchases (US\$ 2.931 million) and system converters (US\$ 1.964 million). The LCOE is the ratio of the total annual cost and total energy produced [44]. The LCOE is calculated as follows [45]:

$$\text{LCOE} = \frac{C_{\text{an,tot}}}{L_{\text{elec}} + E_{\text{gs}}} \quad (5)$$

where $C_{\text{an,tot}}$ is the total annualized cost of the system, L_{elec} is the total electrical load served per year, and E_{gs} is the energy sold to the grid. The LCOE for the proposed NZE water treatment plant was calculated to be 4.6 ¢/kWh, quite less than the original price of the government sector.

3.5. Economic and emission comparison with the existing grid-only system

The NPC of the existing water treatment plant with a grid-only system is US\$ 12.6 million and the LCOE is 8.5 ¢/kWh. The NPC and LCOE of the proposed NZE water treatment plant are 11.75% and 45.9% lower than the existing grid-only system. A cumulative cash flow diagram of the NZE system and the grid only system is shown in Fig.

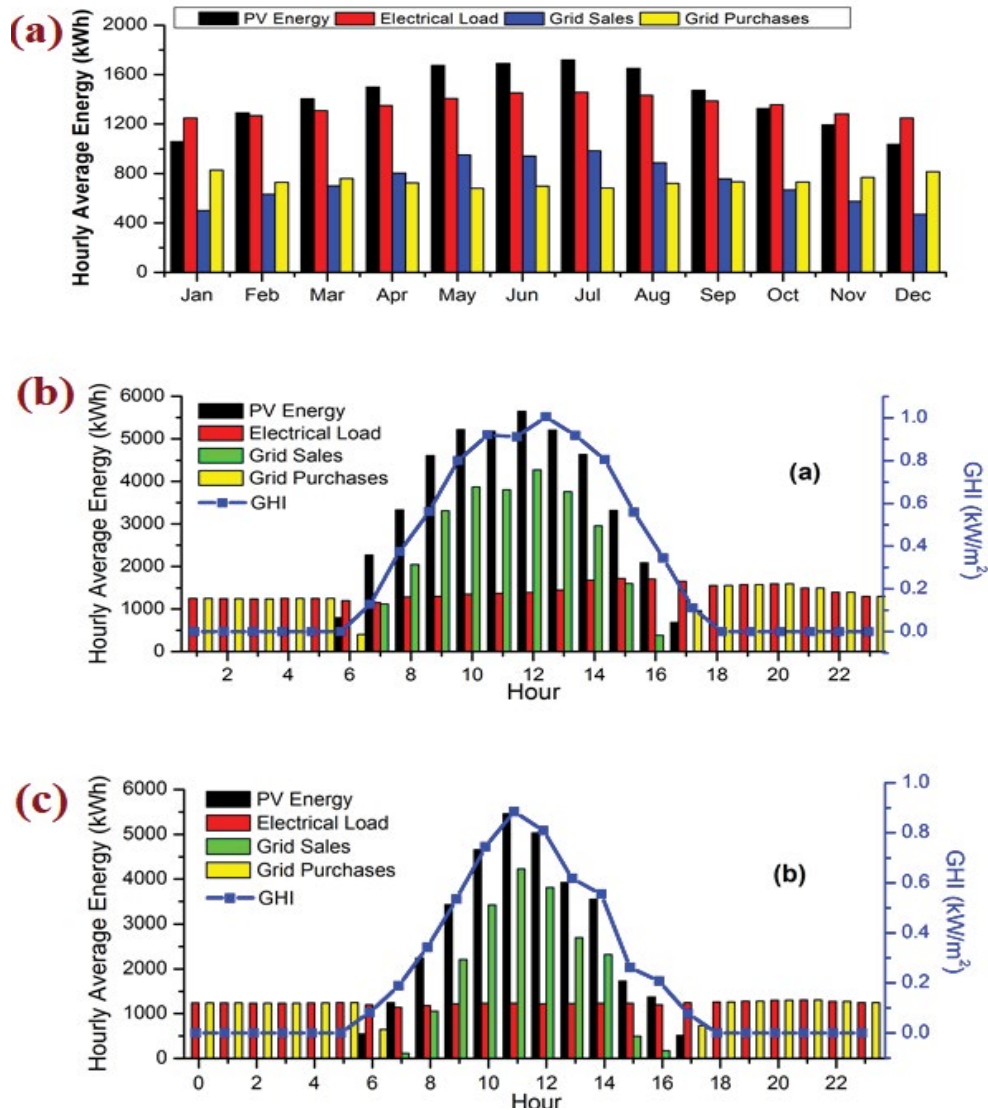


Fig. 11. (a) Hourly average PV energy output, electrical load, grid sales, and purchases. PV energy output, electrical load, grid sales, and purchases for a typical (b) summer day (June 15) and (c) winter day (December 20).

12b. The negative value of the cash of the NZE system in year zero shows the capitals cost of the system (US\$ 7.26 million); however, from year one onward the slope of the grid-only system is steeper than the NZE system because all of the energy is purchased from the grid in the grid-only case. A dip in the cash flow of the NZE system during year 15 shows the replacement cost of the system converters and the positive slope during year 25 of the NZE system shows the revenue generated by the salvage value of the components at the end of the project lifespan. It can be observed in Fig. 12b that the negative cumulative cash flows of the NZE become less than the existing grid-only system. The negative cumulative cash flows of the NZE require 9.67 y to overcome the existing grid-only system and this is the payback period of the proposed NZE system. The LCOE of the proposed NZE water treatment plant is 4.6 ¢/kWh compared to 8.5 ¢/kWh for the existing plant. This is a reduction of 45.9% in the LCOE. This economic comparison to the existing grid-only

Table 7
Costs of various components of the NZE system

Component	Cost	Unit
PV module	1,000	US\$/kW
System converter	150	US\$/kW
Balance of system equipment	100	US\$/kW
Operation and maintenance cost	10	US\$/kW/y
Grid electricity purchase rate	8.5	US\$ ¢/kWh
Grid electricity sales rate	5	US\$ ¢/kWh
Sale tax	5	%

system shows that the proposed NZE system for the water treatment plant is a viable economic option.

The grid-only system produces 7,268.73 tons of carbon dioxide (CO₂), 31.5 tons of sulfur dioxide (SO₂), and 15.4 tons

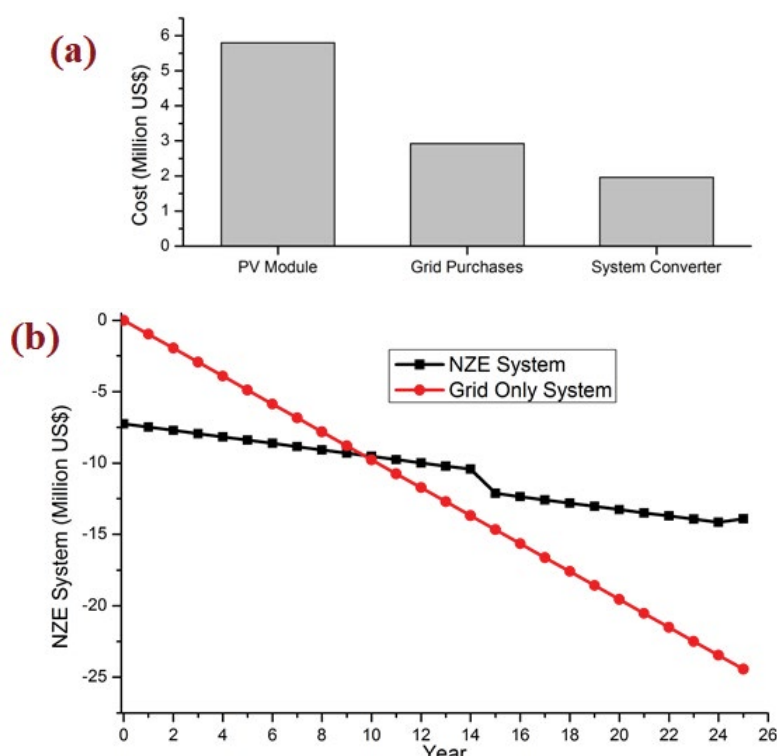


Fig. 12. (a) Costs of various components of the NZE system and (b) cumulative cash flow analysis of the NZE system and the grid only system.

of nitrogen oxide (NO) per year while the PV-based NZE system produces 100% green energy with no emissions during the operational period of the plant. The NZE system saves 181,718.3 tons of CO₂, 787.5 tons of SO₂, and 385.0 tons of NO emissions during the lifespan of the project.

4. Conclusion

- 827.1 nm PAN-NFs were synthesized using the electrospinning process. A Pan-NF was successfully used for micropollutant removal present in dam and wastewater using the nanofiltration method. The experimental results confirm that PAN-NF has the potential to act as a membrane in water purification.
- Analysis of several water quality parameters in the effluent of the TSTP suggests that the removal percentage of the wastewater pollutants was excellent. However, some recommendations by the local auditor need to be considered for better performance.
- The proposed PV-based NZE system for the water treatment plant resulted in an 11.75% and 45.9% reduction in NPC and LCOE, respectively. The NZE system also saved 181,718.3 tons of CO₂, 787.5 tons of SO₂, and 385 tons of NO emissions during its lifetime.

Acknowledgments

The authors extend their appreciation to the Deanship of Scientific Research at Majmaah University for funding their work under project number (RGP-2019–14).

References

- [1] A. Khatoun, M.K. Uddin, R.A.K. Rao, Adsorptive remediation of Pb(II) from aqueous media using *Schleichera oleosa* bark, *Environ. Technol. Innovation*, 11 (2018) 1–14.
- [2] A. Nasar, F. Mashkoo, Application of polyaniline-based adsorbents for dye removal from water and wastewater – a review, *Environ. Sci. Pollut. Res.*, 26 (2019) 5333–5356.
- [3] M.K. Uddin, S.S. Ahmed, M. Naushad, A mini update on fluoride adsorption from aqueous medium using clay materials, *Desal. Water Treat.*, 145 (2019) 232–248.
- [4] R.A.K. Rao, M. Kashifuddin, Kinetics and isotherm studies of Cd(II) adsorption from aqueous solution utilizing seeds of bottlebrush plant (*Callistemon chisholmii*), *Appl. Water Sci.*, 4 (2014) 371–383.
- [5] M.K. Uddin, R.A.K. Rao, K.V.V.C. Mouli, The artificial neural network and Box–Behnken design for Cu²⁺ removal by the pottery sludge from water samples: equilibrium, kinetic and thermodynamic studies, *J. Mol. Liq.*, 266 (2018) 617–627.
- [6] A.A.H. Faisal, S.F.A. Al-Wakel, H.A. Assi, L.A. Naji, M. Naushad, Waterworks sludge-filter sand permeable reactive barrier for removal of toxic lead ions from contaminated groundwater, *J. Water Process Eng.*, 33 (2020) 101112.
- [7] M.K. Uddin, Z. Rehman, Application of Nanomaterials in the Remediation of Textile Effluents from Aqueous Solutions, S. ul-Islam, B.S. Butola, Ed., *Nanomaterials in the Wet Processing of Textiles*, John Wiley & Sons, Inc., 111 River Street, Hoboken, NJ 07030; USA and Scrivener Publishing LLC, 100 Cummings Center, Suite 541J, Beverly, MA 01915, USA, 2018, pp. 135–161.
- [8] M. Naushad, Surfactant assisted nano-composite cation exchanger: development, characterization and applications for the removal of toxic Pb²⁺ from aqueous medium, *Chem. Eng. J.*, 235 (2014) 100–108.
- [9] M. Naushad, A. Mittal, M. Rathore, V. Gupta, Ion-exchange kinetic studies for Cd(II), Co(II), Cu(II), and Pb(II) metal ions

- over a composite cation exchanger, *Desal. Water Treat.* 54 (2015) 2883–2890.
- [10] M. Naushad, Z.A. AlOthman, Separation of toxic Pb²⁺ metal from aqueous solution using strongly acidic cation-exchange resin: analytical applications for the removal of metal ions from pharmaceutical formulation, *Desal. Water Treat.*, 53 (2015) 2158–2166.
- [11] Z. Su, T. Liu, W. Yu, X. Li, N.J.D. Graham, Coagulation of surface water: observations on the significance of biopolymers, *Water Res.*, 126 (2017) 144–152.
- [12] T. Matsuura, S. Sourirajan, Studies on reverse osmosis for water pollution control, *Water Res.*, 6 (1972) 1073–1086.
- [13] N. Serpone, R.F. Khairutdinov, Application of Nanoparticles in the Photocatalytic Degradation of Water Pollutants, P.V. Kamat, D. Meisel, Eds., *Studies in Surface Science and Catalysis*, Elsevier, Netherlands, 1997, pp. 417–444.
- [14] M. Naushad, G. Sharma, Z.A. AlOthman, Photodegradation of toxic dye using gum arabic-crosslinked-poly(acrylamide)/Ni(OH)₂/FeOOH nanocomposites hydrogel, *J. Cleaner Prod.*, 241 (2019) 118263.
- [15] A. Baeza, A. Salas, J. Guillen, A. Munoz-Serrano, M.A. Ontalba-Salamanca, M.C. Jimenez-Ramos, Removal naturally occurring radionuclides from drinking water using a filter specifically designed for drinking water treatment plants, *Chemosphere*, 167 (2017) 107–113.
- [16] C.T. Kenry, Lim nanofiber technology: current status and emerging developments, *Prog. Polym. Sci.*, 70 (2017) 1–17.
- [17] A. Onur, A. Ng, G. Garnier, W. Batchelor, Engineering cellulose fibre inorganic composites for depth filtration and adsorption, *Sep. Purif. Technol.*, 203 (2018) 209–216.
- [18] U. Baig, A. Matin, M.A. Gondal, S.M. Zubair, Facile fabrication of superhydrophobic, superoleophilic photocatalytic membrane for efficient oil-water separation and removal of hazardous organic pollutants, *J. Cleaner Prod.*, 208 (2019) 904–915.
- [19] J. Lee, J. Yoon, J.-H Kim, T. Lee, H. Byun, Electrospun PAN-GO composite nanofibers as water purification membranes, *J. Appl. Polym. Sci.*, 135 (2018) 45858.
- [20] R.K. Sadasivam, S. Mohiyuddin, G. Packirisamy, Electrospun polyacrylonitrile (PAN) templated 2D nanofibrous mats: a platform toward practical applications for dye removal and bacterial disinfection, *ACS Omega*, 2 (2018) 6556–6569.
- [21] S. Ramakrishna, K. Fujihara, W-E. Teo, T. Yong, Z. Ma, R. Ramaseshan, Electrospun nanofibers: solving global issues, *Mater. Today*, 9 (2006) 40–50.
- [22] S. Thenmozhi, N. Dharmaraj, K. Kadirvelu, H.Y. Kim, Electrospun nanofibers: new generation materials for advanced applications, *Mater. Sci. Eng., B*, 217 (2017) 36–48.
- [23] A.R. Bhatti, Z. Salaman, B. Sultana, N. Rasheed, A.B. Awan, U. Sultana, M. Younas, Optimized sizing of photovoltaic-grid-connected electric vehicle charging system using particle swarm optimization, *Int. J. Energy Res.*, 43 (2019) 500–522.
- [24] M. Zubair, A.B. Awan, A.G. Abo-khalil, NPC based design optimization for a net zero office building in hot climates with PV panels as shading device, *Energies*, 11 (2018) 1–20.
- [25] A.B. Awan, M. Zubair, R.P. Praveen, A.G. Abukhalil, Solar energy resource analysis and evaluation of photovoltaic system performance in various regions of Saudi Arabia, *Sustainability*, 10 (2018) 1–27.
- [26] A.B. Awan, M. Zubair, G.A.S. Sidhu, A.R. Bhatti, A.D. Abu-Khalil, Performance analysis of various hybrid renewable energy systems using battery, hydrogen, pumped hydro-based storage units, *Int. J. Energy Res.*, 43 (2018) 6296–6321.
- [27] A.B. Awan, Optimization and techno-economic assessment of rooftop photovoltaic system, *J. Renewable Sustainable Energy*, 11 (2019) 1–15.
- [28] M. Zubair, A.B. Awan, S. Ghuffar, A. Dawood Butt, M. Farhan, Analysis and selection criteria of lakes and dams of Pakistan for floating photovoltaic capabilities, *J. Solar Energy Eng.*, 142 (2020) 1–10.
- [29] A.B. Awan, M. Zubair, R.P. Praveen, A.R. Bhatti, Design and comparative analysis of photovoltaic and parabolic trough based CSP plants, *Solar Energy*, 183 (2019) 551–565.
- [30] M. Zubair, A.B. Awan, R.P. Praveen, Analysis of PV arrays efficiency for reduction of building cooling load in hot climates, *Build. Serv. Eng. Res. Technol.*, 39 (2018) 1–16.
- [31] S.A. Parekh, R.N. David, K.K.R. Bannuru, L. Krishnaswamy, A. Baji, Electrospun silver coated polyacrylonitrile membranes for water filtration applications, *Membranes*, 8 (2018) 59.
- [32] W. Kong, X. Fu, Y. Yuan, Z. Liu, J. Lei, Preparation and thermal properties of crosslinked polyurethane/lauric acid composites as novel form stable phase change materials with a low degree of super cooling, *RSC Adv.*, 7 (2017) 29554–29562.
- [33] B. Minčeva-Šukarova, B. Mangovska, G. Bogoeva-Gaceva, V.M. Petruševski, Micro-Raman and micro-FT-IR spectroscopic investigation of raw and dyed pan fibers, *Croat. Chem. Acta*, 85 (2012) 63–70.
- [34] R. Bryaskova, D. Pencheva, S. Nikolov, T. Kantardjiev, Synthesis and comparative study on the antimicrobial activity of hybrid materials based on silver nanoparticles (AgNps) stabilized by polyvinylpyrrolidone (PVP), *J. Chem. Biol.*, 4 (2011) 185–191.
- [35] J. Li, S. Su, L. Zhou, V. Kundrát, A.M. Abbot, F. Mushtaq, D. Ouyang, D. James, D. Roberts, H. Ye, Carbon nanowalls grown by microwave plasma enhanced chemical vapor deposition during the carbonization of polyacrylonitrile fibers, *J. Appl. Phys.*, 113 (2013) 024313.
- [36] V.A. Dhumale, R.K. Gangwar, S.S. Datar, R.B. Sharma, Reversible aggregation control of polyvinylpyrrolidone capped gold nanoparticles as a function of pH, *Mater. Express*, 2 (2012) 311–318.
- [37] Indian Standard, Drinking Water – Specification, 2nd Revision, IS: 10500, 2012.
- [38] R. Makungo, J.O. Odiyo, N. Tshidzumba, Performance of small water treatment plants: the case study of Mutshedzi water treatment plant, *Phys. Chem. Earth*, 36 (2011) 1151–1158.
- [39] European Communities (Drinking Water) (No. 2) Regulations (S.I. 278 of 2007), 2007.
- [40] World Health Organization, Water Quality and Health – Review of Turbidity: Information for Regulators and Water Suppliers, 2017.
- [41] A.B. Awan, Performance analysis and optimization of a hybrid renewable energy system for sustainable NEOM city in Saudi Arabia, *J. Renewable Sustainable Energy*, 11 (2019) 1–18.
- [42] Saudi Electricity Company, 2018. Available at: <https://www.se.com.sa/enus/customers/Pages/TariffRates.aspx>
- [43] IRENA, Renewable Power Generation Costs in 2017, International Renewable Energy Agency, 2018, pp. 1–160.
- [44] M. Zubair, A.B. Awan, R.P. Praveen, M.A. Baseer, Solar energy export prospects of the kingdom of Saudi Arabia, *J. Renewable Sustainable Energy*, 11 (2019) 1–9.
- [45] R.P. Praveen, M.A. Baseer, A.B. Awan, M. Zubair, Design, performance analysis and optimization of a parabolic trough based concentrated solar power plant for feasible locations in the Middle East Region, *Energies*, 11 (2018) 1–18.

Supplementary information

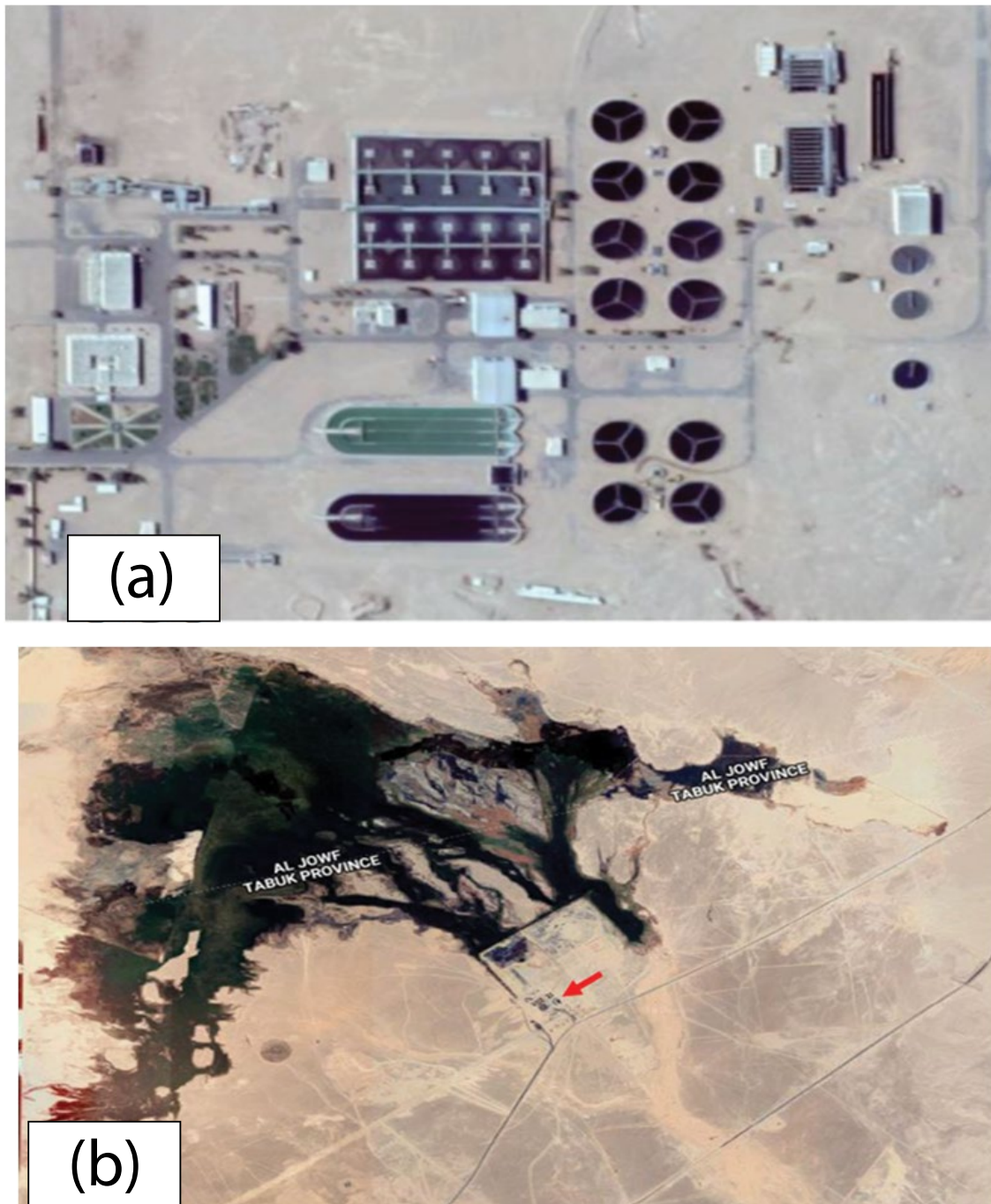


Fig. S1. (a) Geographical location of TSTP and (b) aerial view of TSTP.



Fig. S2. Wastewater before and after treatment stages of TSTP.



Fig. S3. Dam water samples before and after filtration.



Fig. S4. Wastewater samples before and after filtration.